

3D symmetric sampling of sparse acquisition geometries

Gijs J. O. Vermeer¹

ABSTRACT

3D symmetric sampling introduced in the 1990s is characterized by dense sampling of two of the four spatial coordinates. The two sparsely sampled coordinates determine the periodicity of the geometry and the dimension of the offset-vector tiles that can be used to generate pseudocommon-offset-vector gathers. These gathers turn out to be useful for prestack processing applications, such as regularization, migration velocity analysis, and azimuthal anisotropy analysis. Although single-point acquisition is the ideal acquisition method, it is not necessarily better than array-based acquisition. Field arrays are still useful in suppressing noise and need not harm signal in most practical cases. In hybrid geometries three spatial coordinates are sampled densely. In all published cases at least two of the three are sampled quite coarsely and may not provide the best quality for the given trace density. Coil geometry (sailing in circles) is a special case of wide-azimuth towed streamer acquisition. It is essentially a random geometry that should be modifiable into a geometry with regularly sampled midpoints, absolute offsets and azimuths. Despite recent technological developments, the basic idea of 3D symmetric sampling still is a highly useful principle for the design of land and marine 3D seismic surveys.

INTRODUCTION

Symmetric sampling of the seismic wavefield was introduced for 2D lines in Vermeer (1990). The concept is based on a corollary of the reciprocity theorem, which states that the shot gather acquired with the shot at a point P is identical to the receiver gather with the receiver at point P, provided the receivers of the shot gather are replaced by shots in the receiver gather. The validity of the reciprocity theorem is much wider than often assumed; it applies to point sources and point receivers in any elastic medium, be it homogeneous or inhomogeneous, isotropic or anisotropic, (Knopoff and Gangi,

1959; White, 1960; Thomsen, 1999.) As a consequence, the properties of the receiver gather (a collection of many different physical experiments) are the same as the properties of the common shot gather (a single physical experiment). This leads to the requirement that the shots in the receiver gather should be sampled in the same way as the receivers in the shot gather: symmetric sampling of shots and receivers.

The extension of 2D symmetric sampling to 3D is straightforward insofar as 3D receiver gathers and 3D shot gathers are concerned: The sampling requirements of the shots in a 3D receiver gather are the same as of the receivers in a 3D shot gather. However, only in the full 3D geometry with shots and receivers sampled in a regular and dense (x,y) grid will there be fully sampled 3D shot gathers and fully sampled 3D receiver gathers. Only in very rare cases has full 3D been acquired; in most practical cases sparse acquisition geometries are acquired in which at least one, but usually two, spatial coordinates are sampled sparsely. Vermeer (1994, 1998a, 2002) discussed how to extend 2D symmetric sampling to the sampling of sparse 3D geometries.

The objective of this paper is to revisit various subjects discussed in Vermeer (2002) in the light of technological developments over the past 10 years; writing this paper also offers the opportunity to fine-tune some of the insights and recommendations discussed in 2002.

I discuss in some detail: (1) A review of 3D symmetric sampling of most common geometries, (2) processing with offset-vector tile (OVT) gathers, (3) single-point (single sensor and single source) acquisition versus array-based acquisition on land, (4) are hybrid geometries (geometries with three rather densely sampled spatial coordinates) the best way of reducing sparsity?, (5) wide-azimuth towed streamer acquisition with parallel or zigzag geometry, and (6) the design of single-coil geometry. Some remarks are made about simultaneous shooting and random sampling.

REVIEW OF 3D SYMMETRIC SAMPLING OF COMMON SPARSE GEOMETRIES

The most common 3D acquisition geometries are parallel, orthogonal, and areal. Parallel and orthogonal geometries are examples of

¹Manuscript received by the Editor 5 January 2010; revised manuscript received 11 March 2010; published online 22 December 2010.

¹3DSymSam — Geophysical Advice, Oldemarkt, The Netherlands. E-mail: gijs@3dsymsam.nl.
© 2010 Society of Exploration Geophysicists. All rights reserved.

line geometries, in which sources and receivers are sampled densely along the respective acquisition lines, whereas the line intervals correspond to the sparsely sampled coordinates. In parallel geometry, the source and receiver lines are parallel to each other, whereas in orthogonal geometry, source and receiver lines are orthogonal to each other. There are two types of areal geometry. In type 1 the sources are densely sampled in x and y , whereas the receivers are coarsely sampled in x and y ; in type 2 the receivers are densely sampled in x and y and the sources are coarsely sampled in x and y . Type 1 areal geometry sometimes is called node geometry.

Each geometry is (partially) characterized by its basic subset. In the line geometries, the basic subset consists of the combination of all data corresponding to one shot line and one receiver line; i.e., in parallel geometry the basic subset is a midpoint line (the locus of all midpoints that share the same shot line and the same receiver line), whereas in orthogonal geometry the basic subset is the cross-spread (data set with shot line orthogonal to receiver line). In areal geometry type 1, the basic subset is the 3D receiver gather, whereas in areal geometry type 2, the basic subset is the 3D shot gather.

A common feature of these basic subsets is that two of the spatial coordinates are fixed, whereas the other two are densely sampled. Therefore, a common factor in defining 3D symmetric sampling for the three types of geometries is the requirement of proper sampling of the basic subsets of the geometries. Proper sampling is defined as the ability to reconstruct faithfully the underlying continuous wavefield. In array-based acquisition geometries, proper sampling of the desired wavefield also is considered acceptable in 3D symmetric sampling (see below). Proper sampling of the basic subsets implies proper sampling of two of the four spatial coordinates. The other two coordinates will be sampled sparsely, in general.

For each of the three main acquisition geometries, the sampling requirements of the basic subsets have to be supplemented with additional requirements for complete 3D symmetric sampling. In parallel geometry, the additional requirement is to achieve square bins; this is tantamount to a distance between the midpoint lines (= crossline bin size) that is equal to one half of the shot and receiver station intervals. In marine streamer acquisition, 3D symmetric sampling never is achieved because the shot interval always is larger than the receiver station interval. The receiver station interval usually is 12.5 m in modern streamers (or 3.125 m in Q-Marine), whereas the interval between shots tends to be at least 18.75 m (larger if more than one source is used or when recording time is long). In marine streamer acquisition, it always is a struggle to get the crossline bin size down to reasonably small values, such as 12.5 m; however, with 50 m between streamers and using two sources, 12.5-m crossline bin size can be achieved, and many surveys have been acquired with these better parameters. It should be possible to acquire parallel geometry on land with 3D symmetric sampling, but often the crossline bin size is chosen larger than the inline bin size.

Orthogonal geometry can be characterized by three pairs of parameters: shot and receiver station intervals, shot and receiver line intervals, and maximum inline and crossline offsets. These pairs determine bin size, unit cell and midpoint area of cross-spread. The aspect ratios of these pairs are crossline bin size/inline bin size, receiver line interval/shot line interval, and maximum crossline offset/maximum inline offset. 3D symmetric sampling of orthogonal geometry requires that all three aspect ratios of the geometry are equal to one because in that way inline and crossline direction are treated in the same way.

This implies a wide acquisition geometry. 3D symmetric sam-

pling also requires the geometry to be regular; that means that all cross-spreads of the geometry have same-size midpoint areas and inline and crossline symmetry with respect to the intersection of shot line and receiver line (center-spread acquisition for shots and receivers). With large channel capacities available, no longer is it problematic to acquire orthogonal geometry with 3D symmetric sampling parameters. A beautiful example of this kind of acquisition is described in Girard et al. (2007). They use 25-m station intervals, 200-m line intervals and 3000-m maximum offsets. Instead of laying out the nominally required 30 receiver lines with length 6000 m, a super-spread of 33 lines with length 9000 m is used for more efficient acquisition. This led to the acquisition of excess traces, which were not stored on disk.

Areal geometry could be sampled in a way similar to orthogonal geometry. For instance, for type 1 areal geometry the shot station interval can be small in x and y , the receiver grid interval would be large in x and y , and the maximum offsets might be the same in x and y . This again would lead to three aspect ratios — station interval, grid interval and midpoint range of 3D receiver. A geometry equivalent to the example orthogonal geometry of the previous paragraph would consist of 25-m shot sampling intervals in x and y , 200-m grid intervals in x and y , and 3000-m maximum offsets in x and y . However, a better alternative is to use hexagonal sampling of areal geometry. In that case, the midpoint area of a 3D receiver gather has a hexagonal shape so that the ideal of circular symmetry in (x,y) will be approximated more closely, as compared to the square shape of a cross-spread in symmetrically sampled orthogonal geometry.

Sparsity

An important characteristic of all geometries is their degree of sparsity. In orthogonal geometry this is determined by the sampling of the shots in the inline direction — the shot-line interval (SLI), and by the sampling of the receivers in the crossline direction, the receiver-line interval (RLI). The larger the line intervals, the greater the sparsity of the geometry. For a regular geometry, SLI and RLI determine the periodicity of the geometry in the inline and crossline directions, respectively. The area of the unit cell is equal to $SLI * RLI$. Each unit-cell-sized area in the midpoint area of a cross-spread has a limited range of offsets and azimuths and is called an offset-vector tile (OVT, Figure 1). OVT gathers are comprised of corresponding OVTs taken from the cross-spreads in the geometry; these gathers are the single-fold gathers in orthogonal geometry that are nearest to true common offset-vector (COV) gathers. Therefore, these OVT gathers also could be called pseudoCOV gathers. Other authors call them COV gathers or COV cubes (Cary, 1999b; Lecerf et al., 2009). Figure 2 illustrates four OVT gathers taken from a 64-fold geometry. The smaller the line intervals, the closer the geometry is to a full 3D geometry and the closer each OVT gather is to a COV gather.

Note that continuous coverage of an OVT gather requires that the corresponding tile is present in all cross-spreads of the geometry. In a geometry in which not all cross-spreads have the same configuration, some OVT gathers are not complete, and this will lead to potentially serious artifacts in prestack migration of these gathers. Therefore, for optimal prestack migration, the geometry should be regular.

In type 1 areal geometry, the sparsity is determined by the dimensions of the grid cell of the receiver layout (square or hexagonal). Similarly, OVT gathers in this geometry are composed of tiles with the dimensions of the grid cell.

In parallel geometry as recorded in marine streamer acquisition —

narrow or wide — the periodicity of the geometry in the inline direction is determined by the shot-point interval for each midpoint line (this is equal to the shooting interval of the individual source arrays). The periodicity in the crossline direction is formed by the interval between the shot lines of the geometry (for configurations with more than one source array: the interval between sail lines, i.e., crossline roll). In narrow-azimuth streamer acquisition, the crossline fold usually is one, and the crossline roll equals half the width of the streamer

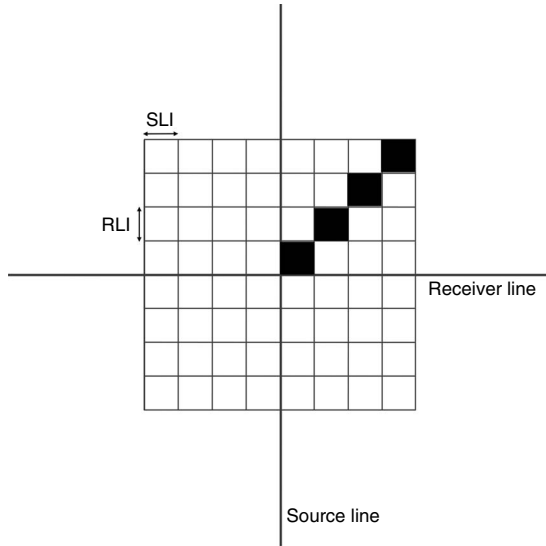


Figure 1. Cross-spread in 64-fold geometry with its 64 unit-cell-sized areas called offset-vector tiles (OVTs). The offset vectors in each OVT have a limited range. The four OVTs in black (with positive inline and crossline offsets) have been selected to generate the OVT gathers shown in Figure 2.

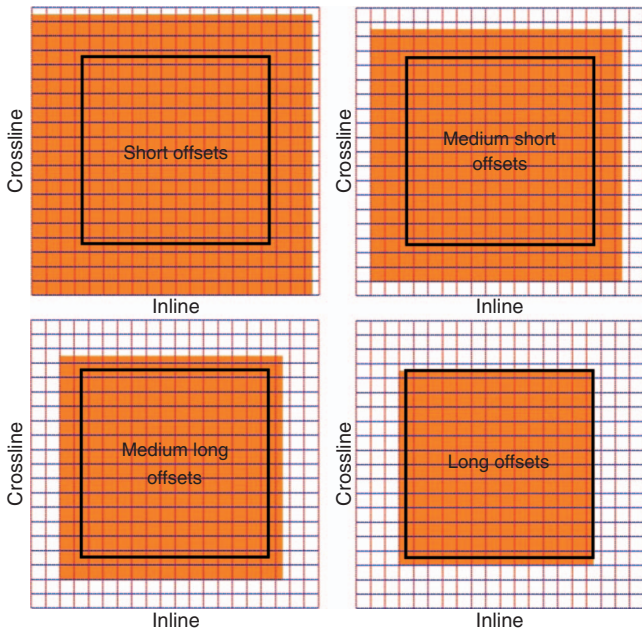


Figure 2. Taking the corresponding tiles from all cross-spreads in this 64-fold orthogonal geometry (shot lines vertical, receiver lines horizontal) produces OVT gathers (in orange) for the four black OVTs in Figure 1. The black square outlines the full-fold area of the geometry.

swath. Therefore, the sparsity of this geometry usually is much larger in the crossline direction — in the order of 500 m — than in the inline direction — in the order of 20 to 40 m. The corresponding OVTs have the same spatial dimensions: very narrow in inline direction and very long in crossline direction.

Reciprocal OVT gathers

Usually, in orthogonal and areal geometry there are shot-receiver azimuths in all four quadrants. This does not lead to reciprocal traces, provided shots and receivers do not occupy the same surface locations. In fact, acquiring data in reciprocal quadrants mitigates the effect of sparsity (see below).

OVTs in a cross-spread located in opposite quadrants that have the same range of absolute inline and crossline offsets might be called reciprocal OVTs (Vermeer, 2007). Figure 3 illustrates reciprocal OVTs. In Figure 3b, the overlapping OVTs do not have reciprocal traces, unless there would be a shot and a receiver at the centers of the two crosses. Instead, the traces of these OVT pairs illuminate the subsurface in a slightly different way. The net result is that reciprocal OVT gathers complement each other’s illumination (see Vermeer, 2002, Chapter 10) and hence mitigate sparsity effects.

Reciprocal OVTs for areal geometry are illustrated in Figure 4. Now the difference in illumination by the two reciprocal OVTs depends on which cluster of shots — area 1 or area 3 for the illustrated OVTs — is shooting downdip or updip.

In parallel geometry, reciprocal OVTs will be acquired with center-spread acquisition (on land) or in some wide-azimuth towed streamer configurations. To mitigate the effect of large crossline rolls in narrow marine streamer acquisition, it has been proposed to use antiparallel acquisition (Vermeer, 1997). However, it would be much better to shoot every line in opposite directions, thus simulating center-spread acquisition. This is illustrated in Figure 5, which shows horizon slices for parallel sailing, antiparallel sailing and center-spread acquisition. Although antiparallel acquisition reduces migration artifacts, center-spread acquisition reduces the acquisition footprint much more because it includes reciprocal OVTs.

An alternative to covering each sail line twice is to deploy a source-only vessel directly behind the streamers of the streamer vessel. This would not increase acquisition time, but would add a source vessel to the total cost. The two or more sources could take turns in shooting, but also could be fired simultaneously. This technique of

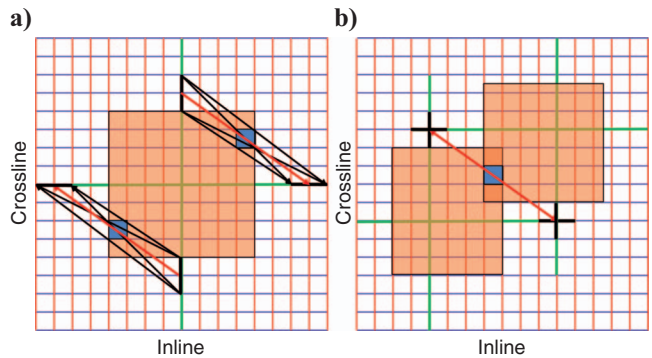


Figure 3. Reciprocal OVTs in 64-fold orthogonal geometry (shot lines red, receiver lines blue), (a) in cross-spread. The red arrows indicate the average offset vector for the two tiles. (b) Overlapping midpoint area of tiles. Note that contributing shots and receivers form two crosses at the endpoints of the red offset vector.

adding a second vessel with one or two extra sources was patented by [Beasley and Chambers \(1999\)](#), precisely in an attempt to overcome the illumination irregularities caused by the large sparsity in the crossline direction. According to [Beasley \(2008\)](#), the industry did not pick up the idea because of the economic downturn. Moreover, the more accessible presentation on simultaneous sources by [Beasley et al. \(1998\)](#), involved a 2D line only; the better illumination for 3D data was not demonstrated and not argued in that paper. With increased confidence that data acquired using simultaneous sources can be separated, this technique might be adopted in the near future. It might turn out that for some areas, center-spread streamer acquisition will obviate the need for the more expensive multi-azimuth acquisition. On the other hand, there is no doubt that multi-azimuth acquisition would also benefit from an extra source vessel behind the streamer swath.

PROCESSING WITH OVT GATHERS

The idea to sort orthogonal geometry data into pseudoCOV gathers and to use them for better prestack migration techniques was thought of independently and almost simultaneously by [Vermeer \(1998b\)](#) and [Cary \(1999a; 1999b\)](#). Implicitly, [Starr's patent \(2000\)](#) also describes the creation and migration of OVT gathers. The patent introduced the sorting of the data inside a bin into inline and crossline offset based on investigation of spider diagrams. The aim of the method was to allow AVO analysis of orthogonal geometry ocean-bottom cable (OBC) data. In Petroleum Geo-Services (PGS), Starr's method is known as common Cartesian offset binning (CCOB).

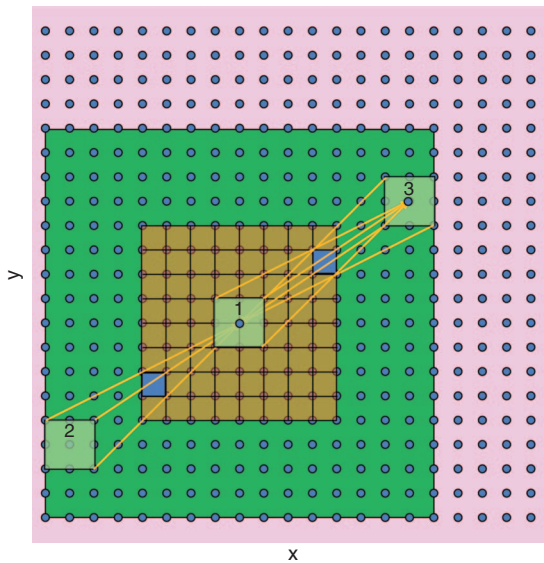


Figure 4. Reciprocal OVTs in Type 1 areal geometry. Each blue circle represents a receiver unit. The whole area is filled with a dense grid of shots. The dark green square represents the area of all shots recorded by receiver 1. The brown square represents the corresponding midpoint area. The shots in area 2 and the shots in area 3 recorded in receiver 1 create a pair of reciprocal OVTs (the small purple squares). These light green shot areas are four times as large as the unit cell (grid cell) of this geometry. The shots in light green area 1 being recorded by receiver 3 create an OVT with the same midpoint area as the OVT created by the shots in light green area 3 recorded by receiver 1.

The industry was slow to adopt the idea of using OVT gathers. Even the highly informative paper by [Gesbert \(2002\)](#) did not lead to widespread followup. Only since 2008, after [Cary and Li \(2005\)](#) presented a paper on regularization using pseudoCOV gathers, and [Vermeer \(2005\)](#) made another plea for OVT-based processing, have many other papers on OVT-gather processing been published. Most of those papers deal with azimuthal anisotropy and in particular with azimuthal velocity analysis in various degrees of sophistication ([Calvert et al., 2008](#); [Bowling et al., 2009](#); [Lecerf et al., 2009](#); [Plasterie et al., 2009](#)). [Plasterie et al. \(2009\)](#), obtain better shallow images

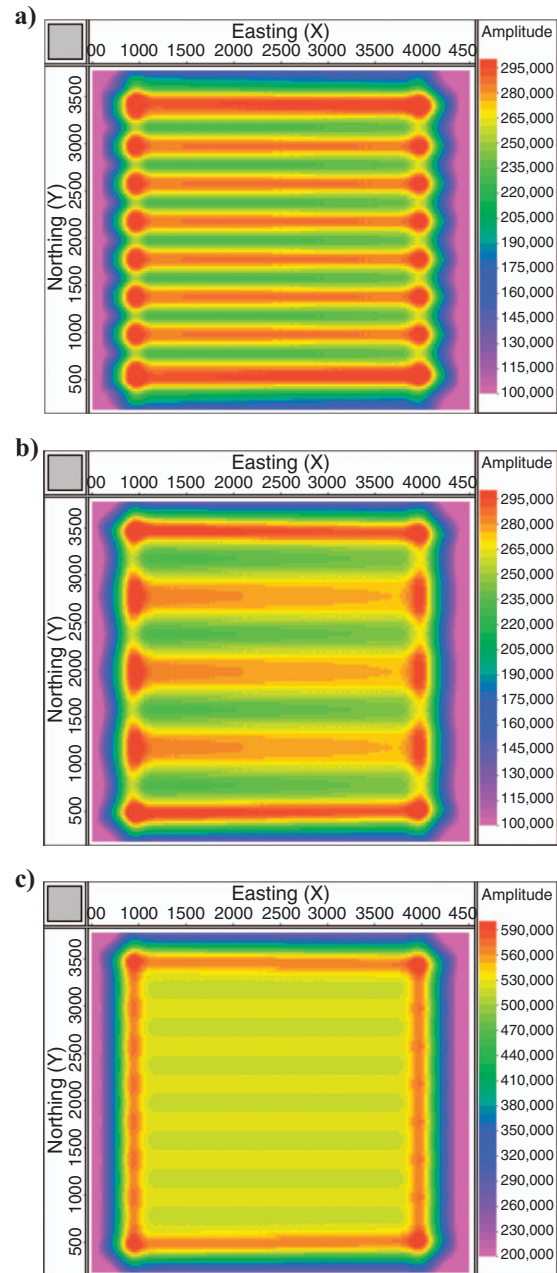


Figure 5. Horizon amplitude slices of migrated pseudoCOV gathers in two sources/eight streamers configuration. The input gathers have a regular midpoint grid of 25×25 m and have inline offsets of 2350 and 2400 m. Reflector dip is 15° . (a) Shooting down-dip, parallel acquisition, (b) antiparallel shooting, (c) center-spread acquisition with use of reciprocal pseudoCOV gathers.

with OVT processing than with absolute offset processing. Figure 6 illustrates azimuthal NMO behavior of a common image gather as discussed in Lecerf et al. (2009). Some papers include azimuthal attribute analysis for reservoir characterization (Boelle et al., 2009; Schapper et al., 2009). Poole et al. (2009) is a very instructive paper on the regularization of data using pseudoCOV gathers.

SINGLE-POINT ACQUISITION VERSUS ARRAY-BASED ACQUISITION ON LAND

Effect of arrays on signal

Proponents of single-sensor and single-source acquisition often spell the big disadvantages of using field arrays (Tessman et al., 2004; Ait-Messaoud et al., 2005). Because acquiring seismic data with field arrays is a requisite to compensate for coarse sampling, it is geophysically more attractive to acquire single-sensor and single-source data without aliasing of the noise. Yet the disadvantages of arrays can be overemphasized as well, and that is what tends to happen. Therefore, it is useful to try and put things into perspective.

The negative effects of arrays on signal are suppression of high frequencies by intraarray statics, and by using too long arrays, and azimuthal effects. The following deals with the first two of these points (azimuthal effects on signal are not really important, provided short arrays are used).

In certain areas, intraarray statics can be the most important source of signal distortion by arrays. The larger the statics between the array elements, the more degradation of signal takes place; the degradation is most serious for the high frequencies. This is illustrat-

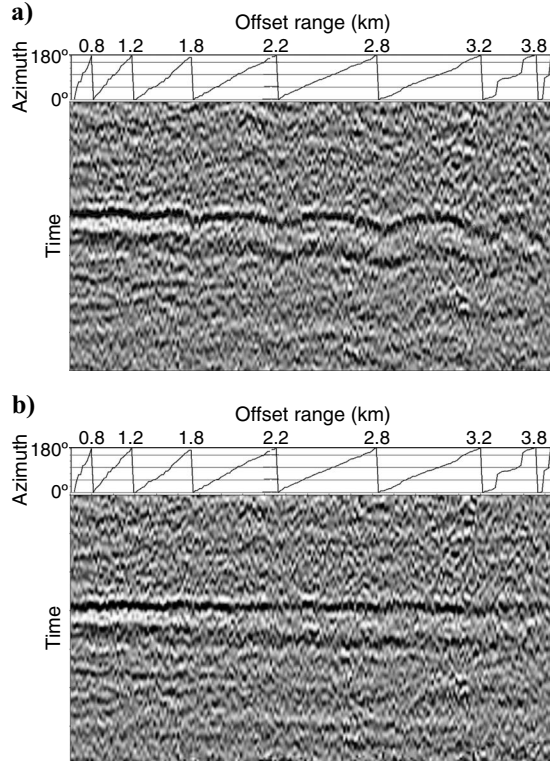


Figure 6. Common-image gather (CIG) with increasing azimuth within each offset range (500 ms time window). (a) Before azimuthal residual moveout, (b) after azimuthal residual moveout using parabolic elliptical model (from Lecerf et al., 2009).

ed in Figure 7, where loss of amplitude in dB is plotted against the standard deviation in the static shifts across the array. Apart from the statics, the computation assumed that the signal arrives at all array elements at the same time, i.e., the computed effects are independent of array length. For a standard deviation of only 2.5 ms, there already is an 8 dB loss in amplitude for 80 Hz.

Intraarray statics tend to be most serious in areas with strong elevation differences. There the best solution would be to locally adapt the station interval and corresponding array length; unfortunately, most recording instruments do not allow a variable number of receiver stations in the spread. A feasible solution would be to preselect the number of receivers in a spread larger than the number required for the nominal geometry. Shot station intervals might be halved easily and the corresponding shots can be labeled A and B. Only in areas with severe statics everywhere is it necessary to use single-sensor acquisition. A nice example with strong static variations resulting from permafrost variations is discussed in Strobbia et al. (2009). Figure 8 is taken from their paper and provides a convincing argument in favor of single-sensor acquisition in areas with large and rapidly varying statics.

To investigate the effect of array length on signal, I have computed the 2D array response for a 12-element linear equidistant array for various values of $f\Delta r/V_{\text{int}}$, where f is frequency, Δr is array length (or station interval, see below), and V_{int} is interval velocity by replacing (apparent) wavenumber k by $f \sin i / V_{\text{int}}$, where i is the reflection angle (assuming horizontal layering). The result is shown in Figure 9. If the station interval is chosen according to the formula $\Delta r = V_{\text{int}} / (2f_{\text{max}} \sin \theta)$ (a commonly used equation for sampling interval, where f_{max} is the maximum frequency in the recorded data), and the angle θ is chosen to be 30° , then $f_{\text{max}} \Delta r / V_{\text{int}} = 1$. The corresponding (dashed) curve shows that the maximum frequency would be suppressed nearly 12 dB for a reflection angle of 50° . The dominant frequency, if taken to be $f_{\text{max}}/2$, would be suppressed less than 3 dB at 50° . This shows that for this choice of station interval the array effect is relatively small, although not negligible. For AVO analysis up to 30° the effect is negligible.

However, station intervals often are chosen much larger than according to the above formula; especially for small dips, θ tends to be

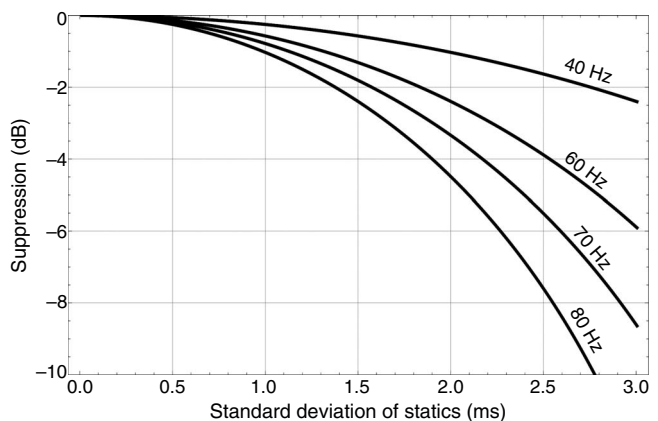


Figure 7. Effect of intraarray statics on frequency content of signal. These curves were computed for a linear distribution of statics (constant slope case); the average of many random statics drawn from a uniform distribution produced very similar curves. D.J. Monk (personal communication, 2010) derived a formula for a normal distribution of statics and found slightly different results with the same message.

chosen smaller than 30° . Even a 50% larger station interval ($f\Delta r/V_{\text{int}} = 1.5$) produces a dramatic loss of high frequencies. This analysis emphasizes the dangerous effect arrays could have on signal amplitude. It strongly underlines the necessity of choosing smaller than usual station intervals. However, if the station spacing is selected smaller than the sampling interval required for alias-free sampling of the prestack data of interest, then the effect of the array on signal is negligible.

Effect of arrays on noise

The array response $p(k)$ of a linear array (array elements arranged along a straight line) is given as

$$p(k) = \frac{\sum_{j=1}^N w_j \exp(2\pi i k x_j)}{\sum_{j=1}^N w_j}, \quad (1)$$

where N is the number of elements in the array, w_j and x_j are the weight factor and location of element j , and k is wavenumber. If the array elements are equidistant with distance d , and the weight factors all are equal, the response simplifies to

$$p(k) = \frac{\sin(N\pi kd)}{N \sin(\pi kd)}. \quad (2)$$

Ongkiehong and Askin (1988) and Vermeer (1990) discussed that the array length ($= Nd$) should be equal to the station interval, even though the first notch of the array response would appear at $k = 1/(Nd) = 2k_N$. Ideally, the response of an array should be equal to that of a spatial antialias filter as can be applied digitally in processing in case of single-sensor recording. Such a filter would have a passband for $k < k_N$ and a reject band for $k > k_N$. A field array also is meant to be an antialias filter, but its response is not flat for $k < k_N$ and there are serious side lobes for $k > 2k_N$.

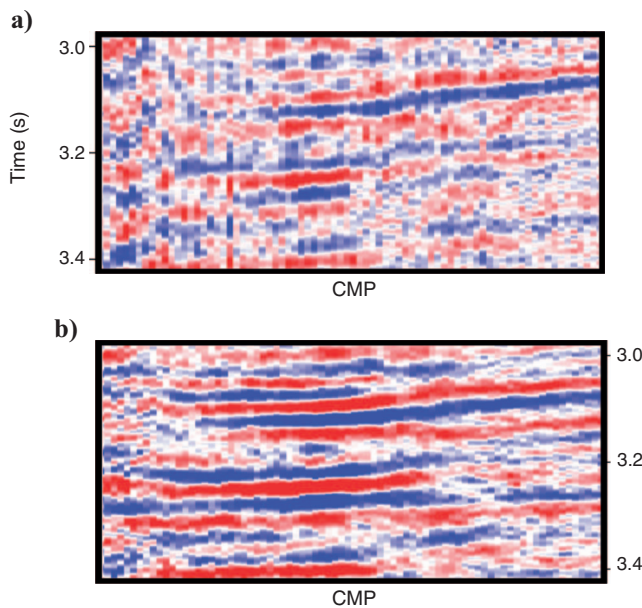


Figure 8. Comparison array-based acquisition with single-sensor acquisition in Arctic. (a) Stack based on simulated 20-m array, (b) stack based on single-sensors with 5-m interval. The big difference between the two results is caused by the large and rapidly varying statics in the survey area (after Strobbia et al., 2009).

Figure 10 illustrates that the amount of noise that can be removed by the combination of field array and velocity filtering could be satisfactory after all. The figure is made for array length = station interval = 25 m, i.e., $k_N = 0.02 \text{ m}^{-1}$. Signal is present in the light-brown area in the f - k domain. There is no aliasing of signal, but various types of noise are aliased. The Rayleigh wave with velocity 600 m/s is aliased above 12 Hz, the refracted S -waves (first arrivals of S) at 33 Hz, and the refracted P (noise following first arrivals) at 60 Hz. All aliased noise is wrapped around to $(-k_N, k_N)$. The figure also shows the response of the field array with length equal to the station interval. This response shows that much of the noise that wraps onto the area around $k = 0$ is removed by the array. Noise in the side lobes is wrapped back to the areas around $k = \pm 0.02 \text{ m}^{-1}$. Therefore, much of this aliased noise and most nonaliased noise can be suppressed by velocity filtering.

Similar conclusions already were reached in the classic paper by Ongkiehong and Askin (1988), but tend to be forgotten in the light of the ideal of single-sensor acquisition.

Figure 10 was made for an area where the largest apparent velocity of the signal is quite large (6000 m/s). For areas with smaller apparent velocities, the triangular signal area expands to larger wavenumbers. The general message of this figure remains that the noise, aliased or not, that does not overlap with the signal might be suppressed by the combination of field array and velocity filtering.

The above discussion deals with a linear array that is effective in one direction only. Similar arguments apply to the combination of two linear arrays — receiver array and shot array — in orthogonal geometry. An exception is scattered noise; this noise requires areal geophone and/or areal shot arrays for best suppression.

Summarizing this section, I assert that although single-point acquisition is the geophysically ideal technique, in many cases array-based acquisition will deliver comparable quality, provided the array lengths are chosen equal to the station intervals and the station intervals are chosen small enough to prevent aliasing of the desired signal. Only in areas with large and rapidly varying statics, or in case really high frequencies ($> 110 \text{ Hz}$) are required (Baeten and van der Heijden, 2008), is single-point acquisition called for. In all other situations, it is more a matter of cost in deciding which way of acquiring 3D seismic data would be preferable.

ARE HYBRID GEOMETRIES THE BEST WAY TO REDUCE SPARSITY?

A hybrid geometry can be considered a combination of orthogonal, areal and parallel geometries. For instance, using dense inline sampling of the receivers of an areal geometry (seabed cable used with dense receiver stations) turns the areal geometry into a hybrid geometry. A properly sampled hybrid geometry would have three properly sampled basic subsets: the midpoint line (parallel geometry), the cross-spread (orthogonal geometry), and the 3D receiver (areal geometry). Typically, hybrid geometry has three densely sampled spatial coordinates and one sparsely sampled spatial coordinate. In all examples known to me, the crossline receiver coordinate is the sparse one.

The first hybrid geometry was a 4C OBC survey acquired by Statoil over the Statfjord field (Rognø et al., 1999). Other hybrid OBC surveys are reported for the Caspian Sea Azeri and Gunashli fields in Bouska and Johnston (2005), and for the North Sea Hild field in Vaxelaire et al. (2007). Hybrid geometry also was acquired in the Life of Field Seismic (LoFS) across Valhall in the North Sea (Kommedal et

crossline source sampling interval, thus achieving square offset-vector tiles. Simultaneous sources in areal WATS would decrease the inline sampling interval, but would not address the larger problem of the coarse crossline source sampling intervals. The second suggestion is to use a zigzag geometry (zigzag WATS), with as many as three source vessels using simultaneous sources; one of the vessels has to cross the streamer swath. For further details the reader is referred to Vermeer (2009).

THE DESIGN OF SINGLE-COIL GEOMETRY

The coil shooting technique was introduced by Moldoveanu (2008). It is a revival of the circle shooting technique tried in the 1980s (French, 1984; Cole and French, 1985). This technique had two main objectives (French, 1984). One main objective was to create controlled feathering, instead of the uncontrollable random feathering that made 3D marine data acquisition using a single streamer very problematic. The other main objective was to do away with the loss of time involved with line turns.

The objective of coil shooting is to cover a large area with a complete range of azimuths. It’s called “coil shooting” because the sail path of the source looks like a coil. At the time of writing, a few tests of this geometry have been acquired. Moldoveanu et al. (2008), and Ross (2008) describe one test; Houbiers et al. (2009) describe a test offshore Norway. One true coil survey has been acquired in Indonesia (Buia et al., 2009a, 2009b; Tozzi et al., 2009). Coil survey design is described in Hill et al. (2009), and in Hill (2009). A coil shooting technique with two streamer vessels and two source vessels has been proposed as well (Moldoveanu and Kapoor, 2009). With this technique, even longer offsets can be acquired for all azimuths.

The beauty of the coil shooting technique is that it does not lose time on line turns; moreover, it acquires long offsets for all azimuths. Yet there are some downsides. Figure 11, adapted from Hill (2009), illustrates the typical coverage that can be obtained with a coil geometry. In the “full-fold” area of this geometry, fold is highly variable. This geometry has a periodicity in x and y , corresponding to the x - and y -increment of the circle centers (typically in the order of 1000–1500 m). In the example of Figure 11, the circle centers are staggered, as can be seen from the periodic pattern in the full-fold area. It should be realized that the pattern of the fold plot in Figure 11 becomes much more erratic when feathering is taken into account.

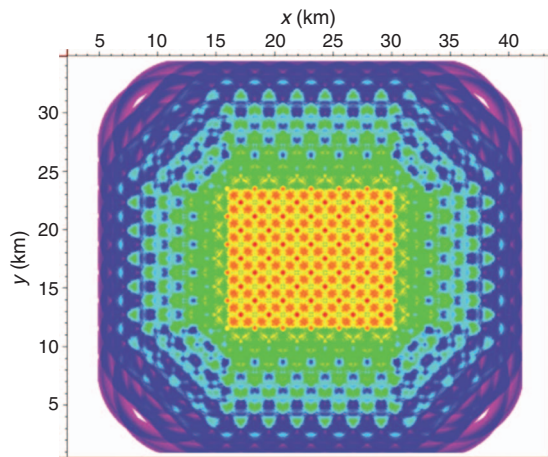


Figure 11. Typical fold of coverage with coil geometry (adapted from Hill, 2009).

Fold in this geometry has to be measured in some square bin, because in streamer acquisition the crossline bin size always differs from the inline bin size, and in this geometry the inline direction keeps varying. Average fold in the full-fold area could be computed from $Fold_{av} = \text{number of shots along circle} * \text{nr of traces per shot} * \text{bin size/area of unit cell}$, or

$$Fold_{av} = 2\pi R/\Delta s * N_c L_c / \Delta r * b_x b_y / (\Delta c_x \Delta c_y), \quad (3)$$

where R is radius of circles, Δs is shot increment, N_c is number of cables, L_c is cable length, Δr is receiver interval, b_x and b_y are bin dimensions in x and y , and Δc_x and Δc_y are the increments (rolls) in x and y of the circle centers. Note that average fold does not depend on streamer interval. As an example — similar to base geometry used in Hill, 2009 — take $R = 5600$ m, $\Delta s = 25$ m, $N_c = 6$, $L_c = 6000$ m, $\Delta r = 12.5$ m, $b_x = b_y = 12.5$ m, $\Delta c_x = 1600$ m, and $\Delta c_y = 1400$ m, would give $Fold_{av} = 377$.

Ross (2008) shows an interesting comparison between typical offset distributions as in areal WATS and in this circular WATS (see Figure 12). The areal WATS shows a regular pattern with dense sampling along vertical lines (the inline direction) and coarse sampling in the crossline direction. The coil shooting also shows clustering along lines, but now in a large variety of directions. Another essential difference between the two geometries is that in areal WATS, trace density (as a function of absolute offset) increases with increasing absolute offset, whereas in the coil geometry trace density is constant nearly for the whole offset range as in 2D acquisition. This shows in Figure 12b as a black area in the center of the plot.

Azimuth clustering is illustrated in Figure 13 for the base geometry of Hill (2009). This geometry has two sources and six streamers with 100 m separation, and streamer length 6000 m. Figure 13a shows a fold plot for the nearest offsets; it shows that the circle centers are arranged in a nearly hexagonal pattern. The overlay shows the huge variation in fold around the average of 377. Figure 13b-d show fold plots for $2 \times 20^\circ$ azimuth sectors for the longest offsets. Opposite azimuths — coming from opposite sides of each sail-line circle — might overlap completely, partially, or not at all. All three azimuth/fold plots show overlap (up to 16 fold) and large areas with zero fold as well. Expected average fold is in the order of 1.4. Smaller circle center intervals and wider swaths would be needed to ensure complete azimuthal coverage, also for the clustered azimuths parallel to the lines of circle centers as in Figure 13b and c.

In the coil geometry, there is regularity in the receiver sampling along the streamers, and in the source sampling along the circles. Also, there is regularity in the positions of the circle centers. Howev-

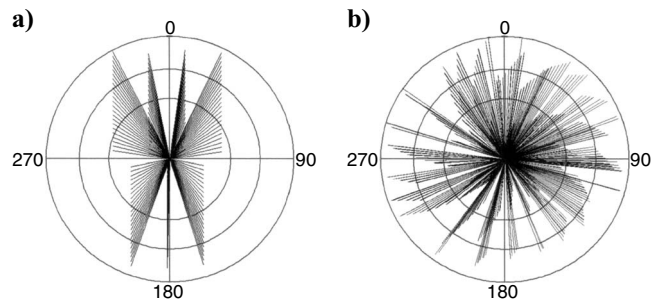


Figure 12. Spider-plot comparison of offset/azimuth distribution in one “full-fold” bin between (a) wide azimuth (WAZ) survey and (b) coil shooting survey. Circles represent constant absolute offset, azimuth is specified in degrees (from Ross, 2008).

er, in x and y the shot and receiver coordinates are highly irregular, and so is the distribution of midpoints. It is not possible to fit circular rings evenly into a square coordinate system. This looks a bit ominous, but the geometry can be regarded also as a random geometry or, with the regularities present in the geometry, a pseudorandom geometry. This means that the geometry should be designed as a random geometry.

The main design criteria for random geometry are that the fold variations should not affect image quality and that illumination is complete. A practical way to realize these criteria is to design such that a well-sampled regular geometry can be reconstructed from the random geometry. In coil geometry, this reconstruction might be carried out in two essential steps, similarly as described in [Poole et al. \(2009\)](#): Interpolate data to a regular grid of midpoints, and then interpolate data in each midpoint to regular polar coordinates.

The first step can be carried out quite easily in the inline direction of each shot-streamer combination; in the crossline direction this could be problematic. Therefore, it would be best to tow the streamers sufficiently close to allow accurate crossline interpolation, and

shoot with one source only. In that way, crossline interpolation to a regular midpoint grid would be most successful.

Polar rather than Cartesian coordinates are most suitable for the second step, because on average each azimuth sector has an equal number of traces that are distributed regularly as a function of offset. The minimum requirements for complete interpolation in each bin depend on the power of the interpolation software, and to some extent on the complexity of the geology, although this latter point is more of influence in the first regularization step. Some trial and error is needed to determine the bins of a geometry with the worst-looking spider plots. If spider plots would look like [Figure 12b](#), then there should be no problem to regularize. Yet, this figure illustrates clearly that interpolating the long offsets is the biggest challenge. An alternative approach to regularization might be the 5D interpolation technique proposed by [Trad \(2009\)](#).

To minimize the gaps in azimuth coverage, the swath should be as wide as possible, and because the streamers have to be close for optimal crossline interpolation, there should be as many streamers as possible. The systematic gaps in azimuth coverage can be removed

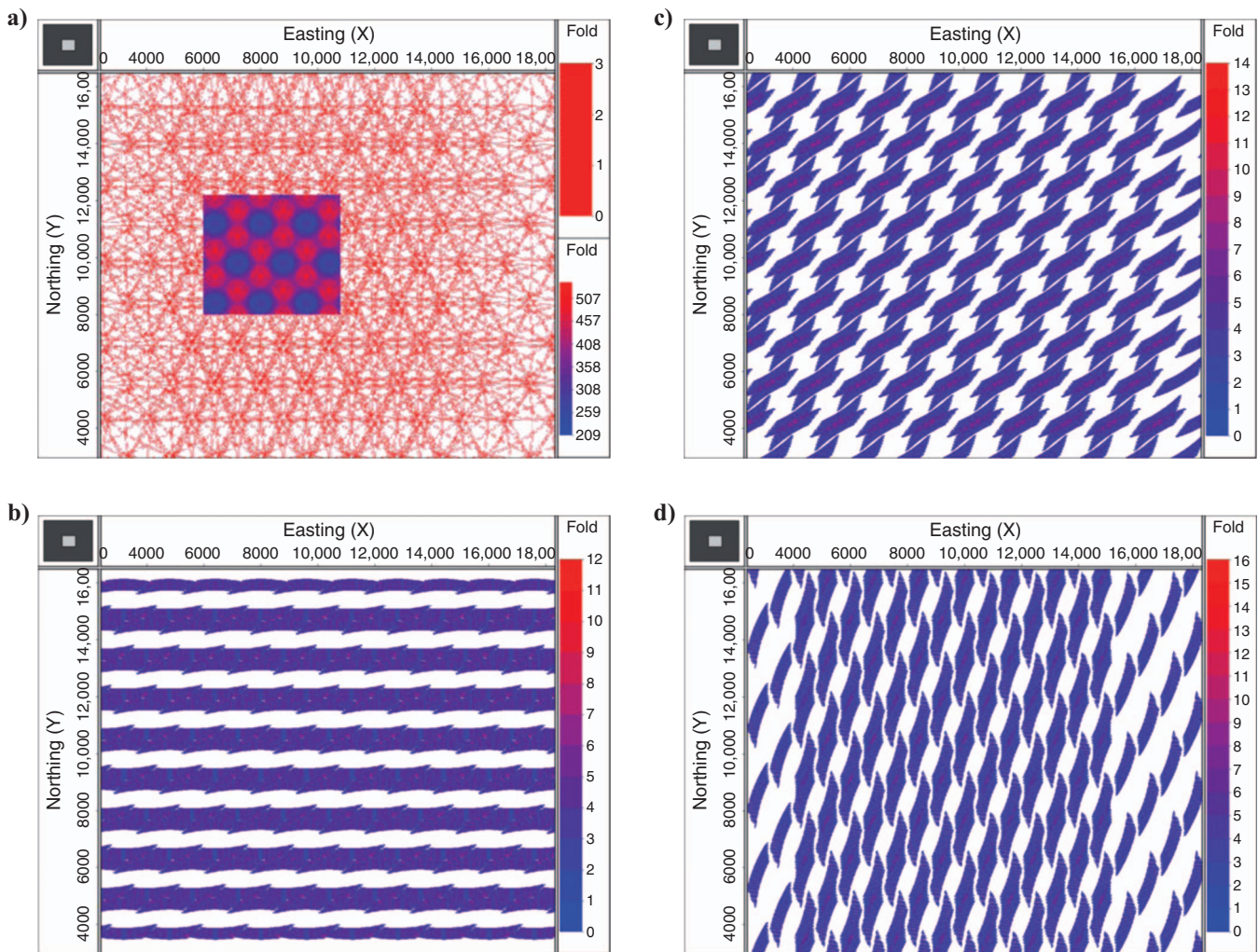


Figure 13. Fold plots for coil shooting with two sources/six streamers configuration; streamer separation 100 m, radius of circles 5600 m, horizontal separation between circle centers 1600 m, vertical separation between horizontal lines of centers 1400 m. (a) All azimuths for very shortest offsets, generated to show triangular circle-center layout, the overlay shows full fold, (b) azimuths from 80° to 100° and from 260° to 280° for offsets 5800 to 6000 m, (c) azimuths from 50° to 70° and from 230° to 250° for offsets 5800 to 6000 m, (d) azimuths from 10° to 30° and from 190° to 210° for offsets 5800 to 6000 m.

by randomizing the locations of the circle centers (Moldoveanu, 2010). Using this approach makes the coil geometry even more like a random geometry.

At the time of writing, there are not yet any coil surveys that have been designed according to these criteria. Yet coil shooting looks like a viable alternative to areal WATS. The technique requires only one streamer vessel and no separate source vessels, and there is no time lost on line turns. An extra advantage of the technique might be the large number of short-offset traces, which might be put to good use in a high fold near-trace cube.

DISCUSSION

Over the past 10 years the available channel counts have increased dramatically. WesternGeco's UniQ has as many as 150,000 channels (WesternGeco, 2009). This allows better sampling, and/or higher fold, and/or more efficient acquisition, the latter especially in combination with simultaneous shooting as described in Bouska (2010). The questions still are how to deploy all those extra channels and in what combination with shots?

It is interesting to approach these questions using OVT gathers as an analysis tool. The hybrid geometry used in Oman's Petroleum Development Oman (PDO) (see Table 1) produces OVTs with size 50×200 m. The offset-vector tiles have two samples at 25 m in the inline direction and four samples at 50 m in the crossline direction. The asymmetry in the offset-vector tiles is caused by the coarse crossline sampling. This might be compared with an orthogonal geometry with the same number of shots but arranged in a 25×100 m grid. In this grid the vibrators would move orthogonal to the receiver lines rather than parallel as in the hybrid geometry; this would have some effect on productivity. The trace density in this alternative geometry is the same, whereas the fold is 1000 in 12.5×12.5 m bins as compared to 4000 in the 25×25 m bins used in the Oman PDO processing (Wombell et al., 2009). The alternative geometry would have OVTs with dimensions 100×200 m, whereas the sampling interval in these OVTs would be 12.5×12.5 m, i.e., symmetric. Thus, not only the cross-spreads would be sampled in a symmetric grid, but also the OVTs, whereas the smaller bin size also should lead to better prestack migration results.

Earlier in this paper I argued that array-based acquisition using alias-free sampling of the desired wavefield should in most cases be as good as single-point acquisition. However, there also is the dilemma of choosing between single-sensor acquisition as promoted by WesternGeco with their Q-Land system or using 3C microelectromechanical system (MEMS) sensors as offered by Ion and Sercel. There is a remarkable discrepancy between the sampling density commonly used in Q-Land versus that used in MEMS 3C acquisition. Typically, in Q-Land four sublimes are used in each receiver line with 12.5 m geophone intervals in each subline. Rached et al. (2009) discuss an example of Q-Land data acquisition in Kuwait with 3840 single sensors per 12 km receiver line. On the other hand, Jianming et al. (2009), describe a 3D/3C MEMS sensor acquisition in Sichuan Basin, China, with 50-m sensor interval and using only 264 3C sensors per 13.2 km receiver spread. This represents a factor 16 (!) difference in sampling density. Of course, there is a large difference in geophysical problems between the two areas, and 3C sensors might be more powerful than 1C sensors. See for instance Diallo and Ross, 2009, for very successful single 3C sensor ground-roll removal.

Another main difference is the philosophy. In Q-Land the objective is to sample the vertical wavefield without aliasing, whereas us-

ers of MEMS might aim for a just-right sampling density of the 3C wavefield (where I can hardly believe that 50-m sampling is just right; denser sampling should produce more reliable results).

The pseudorandom sampling implied by coil shooting requires the ability to reconstruct regular geometry. The narrow-azimuth offset distribution corresponding to each shot means that this regular geometry would be a multiazimuth survey. For instance, it might be decided to split the azimuth range into nine 20° azimuth sectors. These sectors should preferably be the same in all bins to avoid spatial discontinuities. This means that the simulated regular geometry would consist of nine 3D surveys acquired with closely spaced 2D lines — this is the ideal parallel geometry: repeated 2D lines. From these interpolated data true COV gathers can be retrieved.

Coil geometry designed and executed according to the requirements for regularization is very expensive. On the other hand, all other marine streamer acquisition suffers from illumination irregularities resulting from feathering. This applies in particular to the near offsets acquired with a separate source vessel behind the streamers. For more regularity, it is necessary to select an overlap between sail lines that is commensurate with the degree of expected feathering. Further technological developments might make it possible for node acquisition to become the preferred and least expensive solution to acquire high-quality, wide-azimuth 3D marine data.

CONCLUSIONS

3D symmetric sampling prescribes proper sampling of at least two of the four spatial coordinates. The sparsity — and the periodicity — of a geometry is determined by the sampling of the other two coordinates. The general applicability of this approach is underlined by the discussion in this paper. Even the design of coil geometry, a pseudorandom geometry, can be approached on the basis of the symmetric sampling principle.

Using 3D symmetric sampling allows us to split the acquired data into well-sampled, single-fold offset-vector tile gathers. The size of offset-vector tiles is determined by the sparsely sampled spatial coordinates. Offset-vector tile gathers are the nearest to true common offset-vector gathers that can be assembled in sparse geometries. They are useful in regularization, velocity determination and azimuthal anisotropy analysis. The smaller the size of the offset-vector tiles, the better the quality of prestack migration of the seismic data.

The time of array-based acquisition is not over yet, even though proponents of single-point acquisition might claim it is. In most practical cases, array-based acquisition can be as good as single-point acquisition.

The proliferation of hybrid geometries with three densely sampled spatial coordinates has questionable merit, as in most applications at least two of the densely sampled coordinates are too coarsely sampled. It is probably better to carry out proper sampling of two of the spatial coordinates.

In wide acquisition geometries, the sparsity should be the same in x and in y for optimal results. Wide-azimuth towed streamer acquisition based on parallel geometry does not honor this symmetry requirement; instead, it tends to suffer from cost-cutting strategies. Zigzag geometry might be an interesting alternative. Coil geometry is another alternative. In narrow-azimuth marine streamer acquisition, the sparsity is determined by the crossline roll; the negative effects of a large crossline roll can be mitigated by center-spread acquisition.

The best basis for successful noise removal and for high-resolu-

tion imaging ultimately is 3D symmetric sampling with alias-free sampling of two of the four spatial coordinates; for the other two coordinates use sampling intervals that are the same and as small as affordable.

ACKNOWLEDGMENTS

I thank Kees Hornman for a first critical review of this paper and all reviewers of *Geophysics* for their highly constructive remarks. Figures 2, 5, and 13 were made with GEDCO's OMNI Workshop; Figure 7 with Mathematica. I thank EAGE for permission to use Figures 8, 11, and 12, and Total and CGGVERITAS for permission to use Figure 6, which is a product of a joint research project.

REFERENCES

- Ait-Messaoud, M., M.-Z. Boulegroun, A. Gribi, R. Kasmi, M. Touami, B. Anderson, P. Van Baaren, A. El-Emam, G. Rached, A. Laake, S. Pickering, N. Moldoveanu, and A. Özbek, 2005, New dimensions in land seismic technology: Oilfield Review, Schlumberger, autumn 2005, 42–53, http://www.slb.com/~media/Files/resources/oilfield_review/ors05/aut05/p42_53.ashx, accessed 9 September 2009.
- Baeten, G., and H. van der Heijden, 2008, Improving S/N for high frequencies: *The Leading Edge*, **27**, 144–153, doi: 10.1190/1.2840359.
- Beasley, C. J., 2008, A new look at marine simultaneous sources: *The Leading Edge*, **27**, 914–917, doi: 10.1190/1.2954033.
- Beasley, C. J., and R. E. Chambers, 1999, Methods of acquiring and processing seismic data: U.S. Patent 5 924 049.
- Beasley, C. J., R. E. Chambers, and Z. Jiang, 1998, A new look at simultaneous sources: 68th Annual International Meeting, SEG, Expanded Abstracts, 133–135.
- Boelle, J.-L., S. Navion, F. Adler, S. Le Bégat, P. Hugonnet, and K. Kravik, 2008, Seismic imaging improvement thanks to a true wide-azimuth pre-processing sequence applied to a 3D OBC dataset: 70th Conference and Exhibition, EAGE, Extended Abstracts, G016.
- Boelle, J.-L., B. Paternoster, D. Lecerf, S. Navion, A. Belmokhta, and A. Ladmek, 2009, Azimuthal amplitude analysis on data processed in common offset vector domain: 79th Annual International Meeting, SEG, Expanded Abstracts, 1172–1176.
- Bouska, J., 2009, Distance separated simultaneous sweeping: efficient 3D vibroseis acquisition in Oman: 79th Annual International Meeting, SEG, Expanded Abstracts, 1–5.
- Bouska, J., 2010, Distance separated simultaneous sweeping, for fast, clean, vibroseis acquisition: *Geophysical Prospecting*, **58**, 123–153, doi: 10.1111/j.1365-2478.2009.00843.x.
- Bouska, J., and R. Johnston, 2005, The first 3D/4-C ocean bottom seismic survey in the Caspian Sea: Acquisition design and processing strategy: *The Leading Edge*, **24**, 910–921, doi: 10.1190/1.2056392.
- Bowling, J., S. Ji, D. Lin, M. Reasnor, M. Staines, and N. Burke, 2009, From isotropic to anisotropic: Puma/Mad Dog wide azimuth data case study: 79th Annual International Meeting, SEG, Expanded Abstracts, 246–250.
- Buia, M., L. Mapelli, E. Tozzi, T. Bunting, M. Garden, and M. Tham, 2009a, Full azimuth circular survey in Indonesia: Survey design, onboard illumination QC and preliminary processing results: 79th Annual International Meeting, SEG, Expanded Abstracts, 71–75.
- Buia, M., R. Vercesi, T. Bunting, M. Garden, and M. Tham, 2009b, Tulip field 3D coil shooting survey acquisition review: Single vessel full azimuth acquisition offshore Indonesia: 79th Annual International Meeting, SEG, Expanded Abstracts, 66–70.
- Calvert, A., E. Jenner, R. Jefferson, R. Bloor, N. Adams, R. Ramkhalawan, and C. St. Clair, 2008, Wide azimuth imaging and azimuthal velocity analysis using offset vector tile prestack migration: *First Break*, **26**, no. 9, 103–107.
- Cary, P. W., 1999a, Common-offset-vector gathers: An alternative to cross-spreads for wide-azimuth 3-D surveys: 69th Annual International Meeting, SEG, Expanded Abstracts, 1496–1499.
- Cary, P. W., 1999b, Prestack imaging with 3-D common-offset-vector gathers: Crewes research report, <http://www.crewes.org/ForOurSponsors/ResearchReports/reports.php?year=1999>, accessed 7 December 2009.
- Cary, P., and X. Li, 2005, A regularized approach to 3-D prestack time migration: CSEG National Convention, 141–144.
- Cole, R. A., and W. S. French, 1985, A circular seismic acquisition technique for marine three-dimensional surveys: 17th Annual Offshore Technology Conference, paper 4864-MS.
- Diallo, M. S., and W. S. Ross, 2009, Improved adaptive covariance method for 3C polarization filtering and analysis: 71st Conference and Exhibition, EAGE, Extended Abstracts, X034.
- French, W. S., 1984, Circular seismic acquisition system: U.S. Patent 4 486 863.
- Gesbert, S., 2002, From acquisition footprints to true amplitude: *Geophysics*, **67**, 830–839, doi: 10.1190/1.1484527.
- Girard, M., D. Mougenot, C. Paulet, A. Rhamani, J. J. Griso, and Y. Boukhalfa, 2007, Operational implementation of full azimuth, high density land acquisition — 3D Irharen (Algeria): 69th Conference and Exhibition, EAGE, Extended Abstracts, B002.
- Hill, D., 2009, Coil survey design and a comparison with alternative azimuth-rich geometries: *First Break*, **27**, no. 12, 73–82.
- Hill, D. I., G. Brown, R. Campbell, and E. Hager, 2009, A highly efficient coil survey design: 71st Conference and Exhibition, EAGE, Extended Abstracts, V009.
- Houbiers, M., P. Garten, M. Thompson, K. R. Straith, and A. S. Moen, 2009, Marine full-azimuth field trial at Heidrun: 79th Annual International Meeting, SEG, Expanded Abstracts, 1162–1166.
- Jianming, T., H. Yue, X. Xiangrong, J. Tinnin, and J. Hallin, 2009, Application of converted-wave 3D/3-C data for fracture detection in a deep tight-gas reservoir: *The Leading Edge*, **28**, 826–837, doi: 10.1190/1.3167785.
- Knopoff, L., and A. F. Gangi, 1959, Seismic reciprocity: *Geophysics*, **24**, 681–691, doi: 10.1190/1.1438647.
- Kommedal, J. H., O. I. Barkved, and D. J. Howe, 2004, Initial experience operating a permanent 4C seabed array for reservoir monitoring at Valhall: 74th Annual International Meeting, SEG, Expanded Abstracts, 2239–2242.
- Lecerf, D., S. Navion, J. L. Boelle, A. Belmokhtar, and A. Ladmek, 2009, Azimuthal residual velocity analysis in offset vector for WAZ imaging: 71st Conference and Exhibition, EAGE, Extended Abstracts, V013.
- Moldoveanu, N., 2008, Circular geometry for wide-azimuth towed streamer acquisition: 70th Conference and Exhibition, EAGE, Extended Abstracts, G011.
- Moldoveanu, N., 2010, Random sampling: a new strategy for marine acquisition: 80th Annual International Meeting, SEG, Expanded Abstracts, 51–55.
- Moldoveanu, N., and J. Kapoor, 2009, What is the next step after WAZ for exploration in the Gulf of Mexico?: 79th Annual International Meeting, SEG, Expanded Abstracts, 41–45.
- Moldoveanu, N., J. Kapoor, and M. Egan, 2008, Full-azimuth imaging using circular geometry acquisition: *The Leading Edge*, **27**, 908–913, doi: 10.1190/1.2954032.
- Nolte, B., S. Brandsberg-Dahl, R. Clarke, and R. Read, 2004, Decimation tests using Valhall ocean-bottom-cable data: 74th Annual International Meeting, SEG, Expanded Abstracts, 45–48.
- Ongkiehong, L., and H. J. Askin, 1988, Towards the universal seismic acquisition technique: *First Break*, **6**, 46–63.
- Plasterie, P., D. Le Meur, and R. Pillai, 2009, Using modern processing technologies to improve poor signal to noise ratio — A 3D land case study: 71st Conference and Exhibition, EAGE, workshops and field trips, WS 10: Advances in land seismic processing, including near-surface modelling.
- Poole, G., P. Herrmann, E. Angerer, and S. Perrier, 2009, A regularization workflow for the processing of cross-spread COV data: 71st Conference and Exhibition, EAGE, Extended Abstracts, P241.
- Rached, G., J. Al-Genai, and B. Al-Ajmi, 2009, Lessons learned from acquiring and processing a full-azimuth 3D land seismic survey in Kuwait: 79th Annual International Meeting, SEG, Expanded Abstracts, 157–161.
- Rognø, H., A. Kristensen, and L. Amundsen, 1999, The Stafford 3-D, 4-C OBC survey: *The Leading Edge*, **18**, 1301–1305, doi: 10.1190/1.1438204.
- Ross, R., 2008, Full azimuth imaging using coil shooting acquisition: *First Break*, **26**, no. 12, 69–74.
- Sambell, R., S. Al-Mahrooqi, C. Matheny, S. Al-Abri, and S. Al-Yarubi, 2010, Land seismic super-crew unlocks the Ara carbonate play of the Southern Oman Salt Basin with wide azimuth survey: *First Break*, **28**, no. 2, 61–68.
- Schapper, S., R. Jefferson, A. Calvert, and M. Williams, 2009, Anisotropic velocities and offset-vector tile prestack-migration processing of the Durham Ranch 3D, Northwest Colorado: *The Leading Edge*, **28**, 1352–1361, doi: 10.1190/1.3259614.
- Starr, J., 2000, Method of creating common-offset/common-azimuth gathers in 3-D seismic surveys and method of conducting reflection attribute variation analysis: U.S. Patent 6 026 059.
- Strobbia, C., A. Glushchenko, A. Laake, P. Vermeer, T. J. Papworth, and Y. Ji, 2009, Arctic near-surface challenges: the point receiver solution to coherent noise and statics: *First Break*, **27**, no. 2, 69–76.
- Tessman, D. J., M. Bahorich, and D. Monk, 2004, Recent advances in point receiver technology — Are field arrays a requirement any longer?: 66th Conference and Exhibition, EAGE, Extended Abstracts, P-195.
- Thomsen, L., 1999, Converted-wave reflection seismology over inhomogeneous, anisotropic media: *Geophysics*, **64**, 678–690, doi: 10.1190/1.1444577.
- Tozzi, E., M. Buia, and L. Mapelli, 2009, Circular shooting on Tulip field — Full azimuth streamer acquisition and illumination QC: 71st Conference

- and Exhibition, EAGE, Extended Abstracts, V010.
- Trad, D., 2009, Five-dimensional interpolation: Recovering from acquisition constraints: *Geophysics*, **74**, no. 6, V123–V132, doi: 10.1190/1.3245216.
- Vaxelaire, D., K. Kravik, F. Bertini, and J. M. Mougenot, 2007, Wide azimuth 3D 4C OBC — A key breakthrough to lead to the development of Hild Field: 69th Conference and Exhibition, EAGE, Extended Abstracts, C009.
- Vermeer, G. J. O., 1990, Seismic wavefield sampling: SEG.
- Vermeer, G. J. O., 1994, 3D symmetric sampling: 64th Annual International Meeting, SEG, Expanded Abstracts, 906–909.
- Vermeer, G. J. O., 1997, Streamers versus stationary receivers: 29th Annual Offshore Technology Conference, paper OTC 8314, p. 331–346.
- Vermeer, G. J. O., 1998a, 3-D symmetric sampling: *Geophysics*, **63**, 1629–1647, doi: 10.1190/1.1444459.
- Vermeer, G. J. O., 1998b, Creating image gathers in the absence of proper common-offset gathers: *Exploration Geophysics*, **29**, 636–642, doi: 10.1071/EG998636.
- Vermeer, G. J. O., 2002, 3-D seismic survey design: SEG.
- Vermeer, G. J. O., 2005, Processing orthogonal geometry — what is missing?: 75th Annual International Meeting, SEG, Expanded Abstracts, 2201–2205.
- Vermeer, G. J. O., 2007, Reciprocal offset-vector tiles in various acquisition geometries: 77th Annual International Meeting, SEG, Expanded Abstracts, 61–65.
- Vermeer, G. J. O., 2009, Wide-azimuth towed-streamer data acquisition and simultaneous sources: *The Leading Edge*, **28**, 950–958, doi: 10.1190/1.3192843.
- WesternGeco, 2009, Land Q-technology, <http://www.westerngeco.com/services/land/landqtechnology.aspx>, accessed 22 December 2009.
- White, J. E., 1960, Use of reciprocity theorem for computation of low frequency radiation patterns: *Geophysics*, **25**, 613–624, doi: 10.1190/1.1438742.
- Wombell, R. J., R. Smith, P. Zwartjes, T. van Dijk, N. Benjamin, T. Wah Hong, O. Khakimov, R. Cramp, A. McCarthy, and M. Bulteau, 2009, South Oman salt basin — High-density wide-azimuth land seismic acquisition and processing: EAGE, Subsalt imaging workshop: focus on azimuths, SS28.